Chemistry & Biology *17*

Supplemental Information

Discovery and Characterization of 2-Anilino-4-(Thiazol-5-yl)Pyrimidine Transcriptional CDK Inhibitors as Anticancer Agents

Shudong Wang, Gary Griffiths, Carol A. Midgley, Anna L. Barnett, Michael Cooper, Joanna Grabarek, Laura Ingram, Wayne Jackson, George Kontopidis, Steven J. McClue, Campbell McInnes, Janice McLachlan, Christopher Meades, Mokdad Mezna, Iain Stuart, Mark P. Thomas, Daniella I. Zheleva, David P. Lane, Robert C. Jackson, David M. Glover, David G. Blake, and Peter M. Fischer

Table S1a (related to Table 1). *In vitro* kinase selectivity of compound **14**.

Kinase	IC_{50} (μM)[a]
Bcr-Abl	4.4 ± 0.2
Akt/PKB	> 10
CaMKII	> 10
CK2	> 10
ERK-2	> 10
GSK3b	0.39 ± 0.04
Lck	1.9 ± 0.1
PDGFb	0.80 ± 0.09
Plk1	> 10
PKA	> 10
PKC	> 10
S6	8.6 ± 3.7
SAPK2a	> 10
Src	2.0 ± 0.1
VEGFR2	0.18 ± 0.02
Aurora A	0.65 ± 0.06
Aurora B	0.40 ± 0.13

[a] Mean ± SD of at least two independent determinations; [ATP] = 0.1 mM.

Table S1b (related to Table 1). Biopharmaceutical and pharmacokinetic properties of compound **14**.

***In vitro* biopharmaceutical properties**		
Partition coefficient	$LogD_{7.4}$[a]	1.1
Dissociation constants	pK_a[b]	8.3, 3.1
Aqueous solubility[c]		> 100 μM
Intestinal permeability	P_{app}[d] (10^{-6} cm/s)	2.4
Microsomal stability[e]	CL_{int} (mL/min/mg)	27.5
	$t_{1/2}$ (min)	50

Plasma protein binding[f]	Fraction bound (%)	64	
Rat pharmacokinetics			
Pharmacokinetic parameter		5 mg/kg *iv*	50 mg/kg *po*
Exposure	$AUC_{0\text{-}24h}$ (h.μM)	1.5	10.4
Elimination	$t_{1/2}$ (h)	1.0	4.9
Clearance	CL (L/h/kg)	8.7	12.2
Volume of distribution	V_z-F (L/kg)	126	97
Oral bioavailability	(% F)		70

[a] Partitioning between octanol and aqueous buffer using the shake-flask method; [b] determined using a pH-metric method; [c] by turbidimetry; [d] apparent permeability coefficient measured using a Caco-2 cell layer assay; [e] measured by disappearance of parent compound (LC-MS) from a preparation of rat liver microsomes; [f] rat plasma protein binding using an equilibrium dialysis assay.

Table S1c (related to Table 1). Antiproliferative activity of compound **14**.

	Human cell line		**72-h MTT**
	Origin	*Designation*	**IC_{50} ± SD (nM)**
Transformed	Bone osteosarcoma	Saos-2	386 ± 189
		U2OS	372 ± 69
	Breast	MDA-MB-468	221 ± 56
		MCF-7	490 ± 358
	Cervix	Hela	401 ± 154
	Colon	HT29	280 ± 73
		LOVO	218 ± 118
		NCI-H1299	501 ± 207
		HCT-116	180 ± 44
	Gastric adenocarcinoma	AGS	256 ± 104
	Leukemia	CCRF-CEM	577 ± 438
	Promyelocytic leukaemia	HL60	374 ± 25
	Lung	A549	299 ± 93
		NCI-H460	264 ± 146
	Leiomyosarcoma	SKUT-1B	107 ± 43
		SKUT-1	225 ± 75
	Neuroblastoma	SK-N-MC	149 ± 24
	Ovarian carcinoma	A2780	131 ± 9
	Pancreatic carcinoma	Mia-Paca-2	139 ± 9
	Prostate	DU-145	140 ± 17
	Skin keratinocyte	Hacat	351 ± 122
	Uterine	Messa	150 ± 16
		Messa-Dx5	536 ± 260
Untransformed	Foetal lung fibroblast	IMR-90	12,278 ± 1,422
		WI38	5,748 ± 3,123
Mean transformed			293
Median transformed			264
Mean untransformed			9013

Table S2 (related to Figure 3). Selective induction of apoptosis in transformed cells by CDK9-selective compounds.

Treatment		**% Cells TUNEL-positive**[a]	
Test compound	Concentration (μM)	A2780 (Transformed)	WI-38 (Untransformed)
Compound **3**	0.2	8	NT
	1.0	63	3
Compound **9**	1.0	6	NT
	5.0	69	17
Compound **10**	1.0	2	NT
	5.0	53	10
Control		1	0

[a] TUNEL analysis of treated cells. A2780 or cycling WI-38 cells were treated with compounds for 24 h. Cells were analysed for DNA strand breaks by the TUNEL method. The percentages of cells labelled as TUNEL-positive are shown. All compounds show a greater selectivity for the transformed line over the untransformed one. NT-not tested.

Table S3 (related to Figure 4). Data collection and refinement statistics for X-ray crystal structure complexes of CDK2 with compounds **11** and **14**.

Data collection	CDK2-compound **11**	CDK2-compound **14**
Space group	$P2_12_12_1$	$P2_12_12_1$
Unit cell dimensions; a, b, c (Å)	53.12, 71.50, 71.64	53.00, 71.11, 72.03
Maximum resolution (Å)	1.9	1.8
Total observations	67,708	67,264
Unique reflections	21,623	25,565
Completeness (%)	97.9	98.8
R_{merge}	0.078	0.075
$<I / \sigma I>$	7.9	7.3
R_{merge}, highest resolution bin	0.415	0.485
$<I / \sigma I>$, highest resolution bin	2.3	2.1
Refinement		
Protein atoms	2,404	2,487
Ligand atoms	58	54
Water molecules	255	271
Reflections used in refinement	20,724	22,796
R_{work}	18.9	21.1
R_{free}	27.1	29.5
Mean B-factor, protein ($Å^2$)	52.1	48.8
Mean B-factor, ligands ($Å^2$)	57.8	40.2
Mean B-factor, solvent ($Å^2$)	58.5	53.4
Bond lengths from ideal values RMSD (Å)	0.011	0.012

Bond angles from ideal values RMSD (degrees)	1.69	1.60

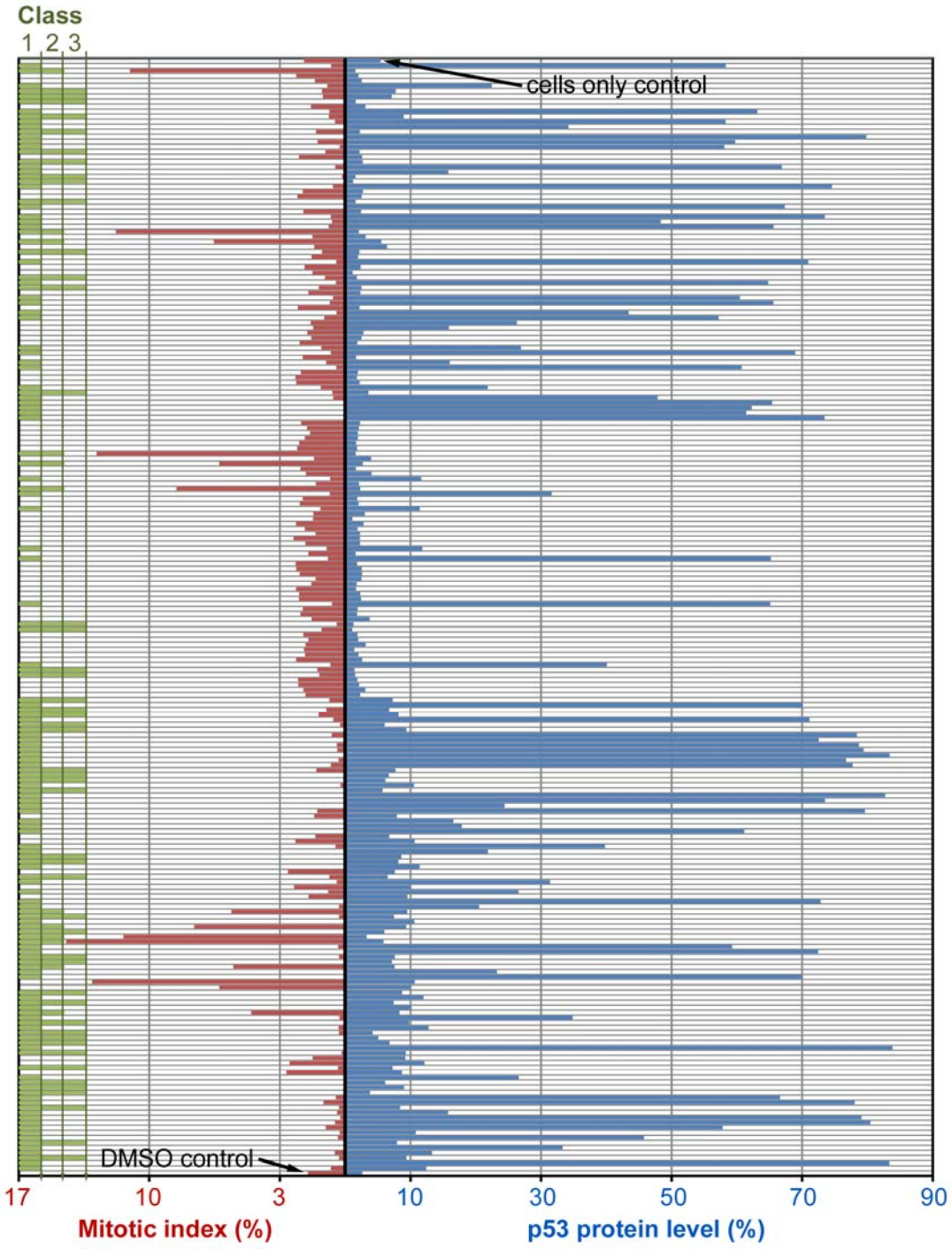

Figure S1a (related to Figure 1). Identification of CDK transcriptional inhibitors by cell-based assays. Cells were treated with a set of 220 test compounds from our 2-anilino-4-(heteroaryl)pyrimidine kinase inhibitor compound library (Wang et al., 2004a; Wang et al., 2004b; Wu et al., 2003) or assay diluent only (DMSO control) at 10 μM for 7 h. MI was measured by determining the percentages of phospho-histone-H3 positive U2-OS cells. Nuclear accumulation of p53 was assessed by immunofluorescent staining in

MCF-7 cells. Phenotypic classification is indicated: unclassified; class 1 (transcriptional inhibitors); class 2 (mitotic inhibitors); class 3 (cell cycle inhibitors).

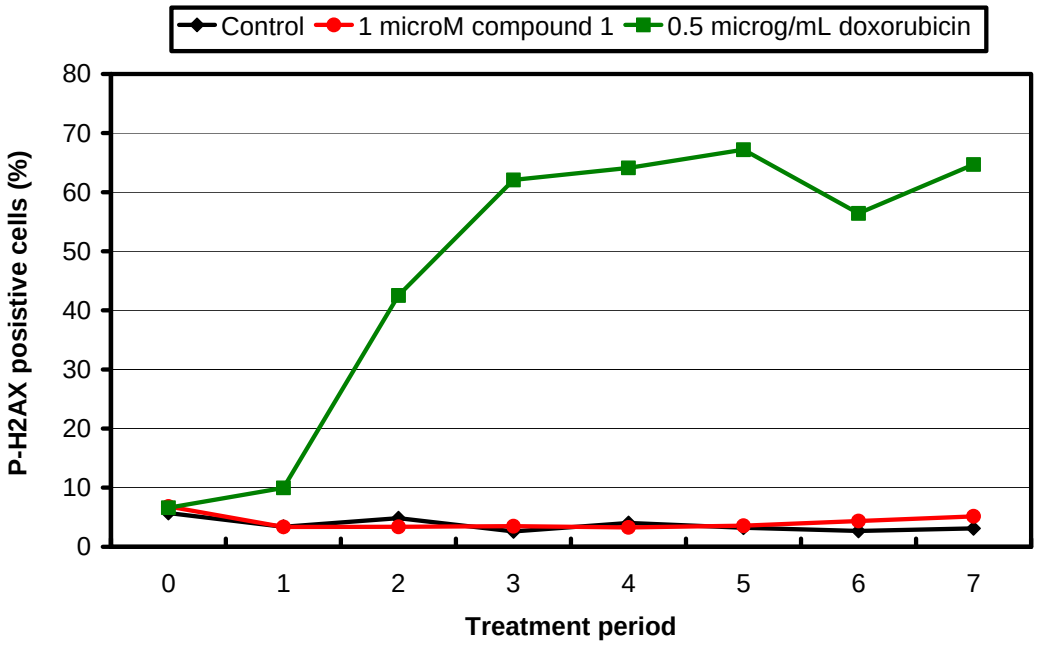

Figure S1b (related to Figure 1). Induction of histone H2AX phosphorylation. Compound **1** does not induce phosphorylation of histone H2AX, (a classical marker of DNA damage) at early time points in contrast to the DNA damaging agent doxorubicin. Cells were treated with compounds or assay diluent only (control) at the concentrations indicated for 7 h.

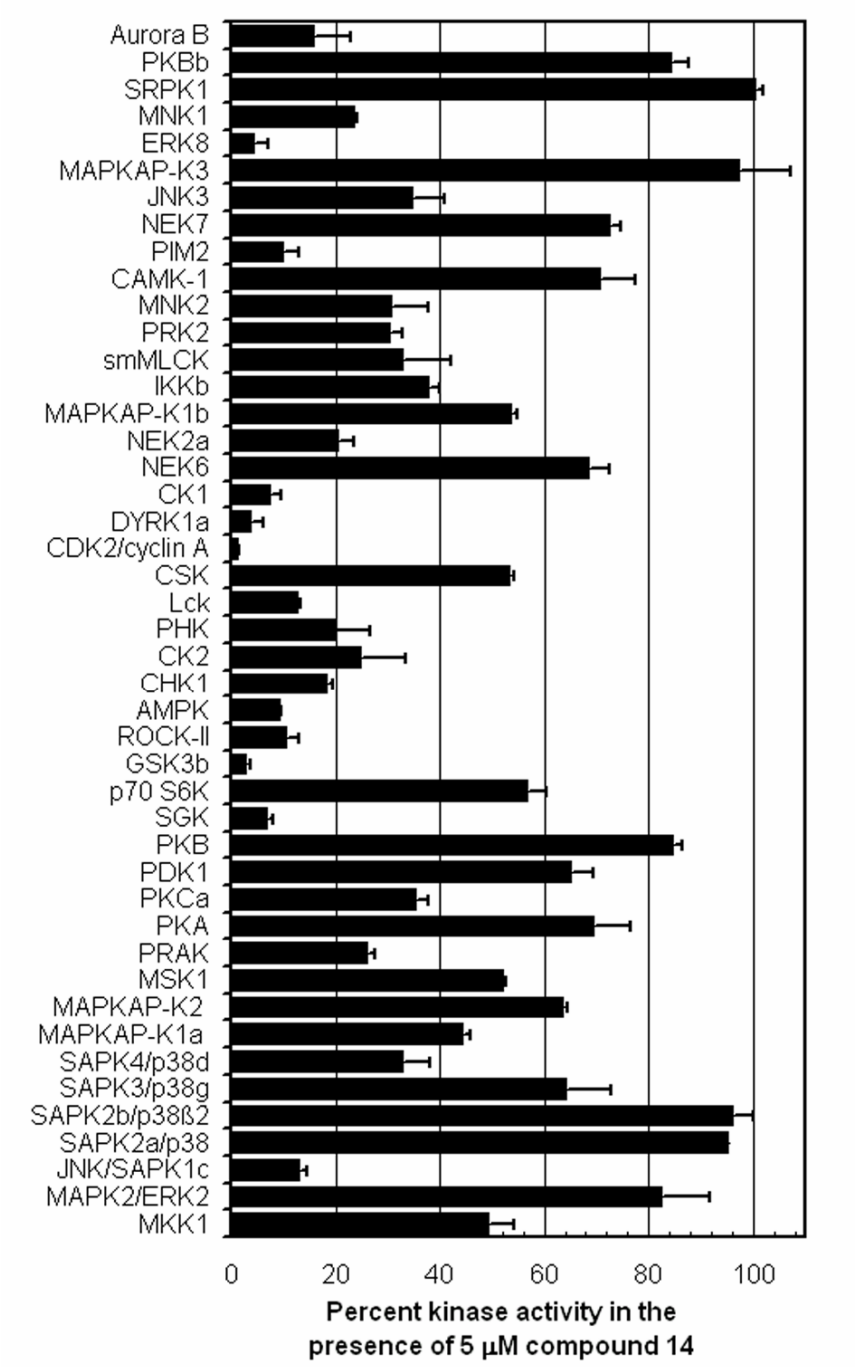

Figure S1c (related to Table 1). Human kinase assay panel for compound 14. The assays were carried out using appropriate protein or peptide substrates and at ATP concentrations near the $K_{m,ATP}$ for the individual kinases (5 – 50 µM).

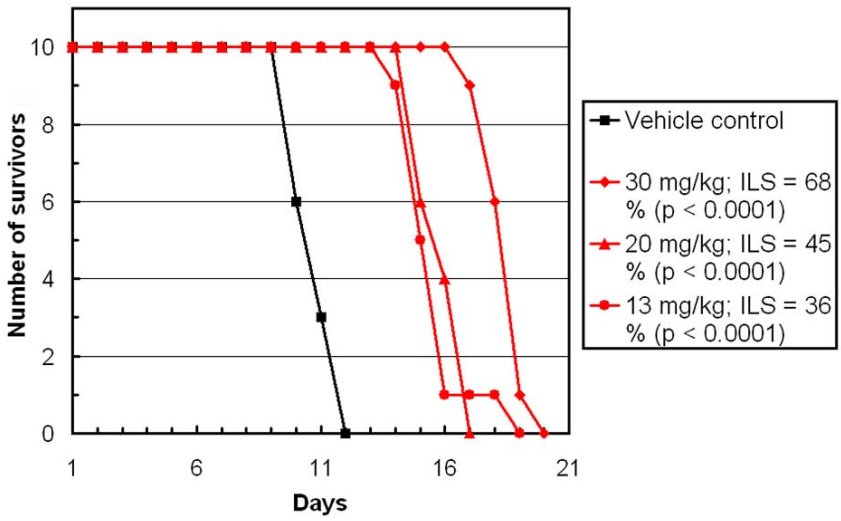

Figure S2a (related to Table 1). ***In vivo*** **antitumour activity of compound 14 in the murine P388/0 survival model.** Groups of animals were dosed *ip* with compound **14** twice daily for ten days.

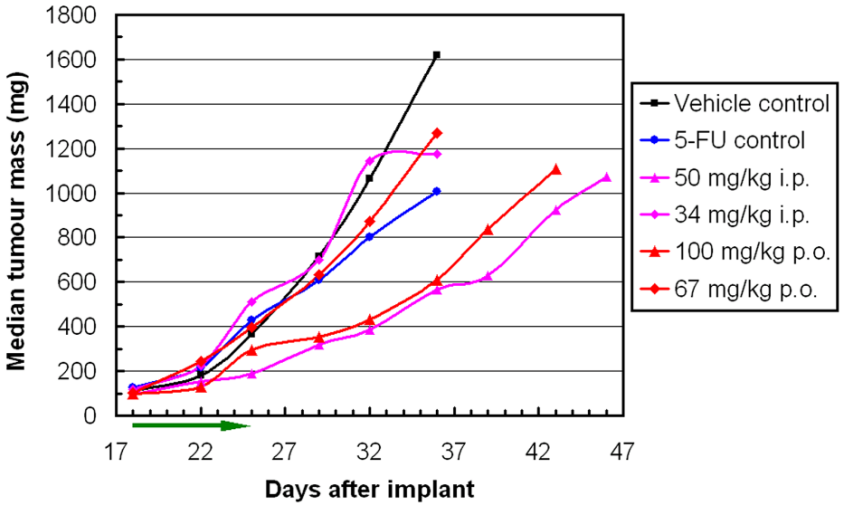

Figure S2b (related to Table 1). ***In vivo*** **antitumour activity of compound 14 in the Colo-205 xenograft model.** Compound **14** was administered once daily for 8 days. The positive control chemotherapy agent 5-FU was given using an optimal dose and schedule for the Colo-205 model. Tumour *versus* control ratios (% T/C) on days 29, 32 and 36: 85, 75 and 62% (5-FU); 45, 36 and 35% (**14**, 50 mg/kg *ip*); 49, 41 and 38% (14, 100 mg/kg *po*). Maximal growth delay (T – C) was 15 days (**14**, 50 mg/kg *ip*) and 12 days (**14**, 100 mg/kg *po*).

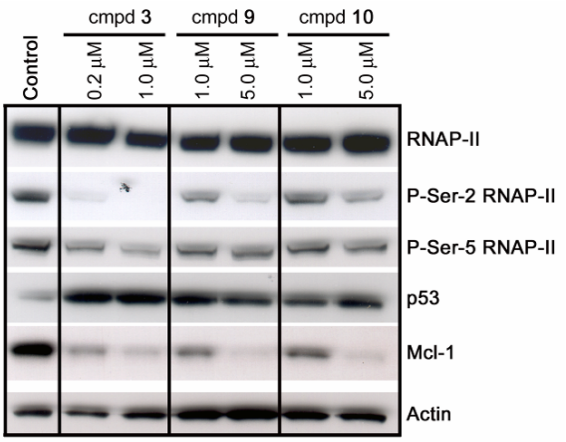

Figure S3 (related to Figure 5). Cellular effects of CDK9-selective compounds. A2780 cells were treated with compounds **3**, **9** and **10** for 3 hours. These compounds represent molecules with a greater selectivity for CDK9 over CDK7 compared to **14**. Each compound can reduce the phosphorylation of RNAP-II CTD at Ser-2, induce p53, and reduce levels of Mcl-1.

Supplemental Experimental Procedures

Synthesis and compound characterisation

3-[4-(2-Ethylamino-4-methyl-thiazol-5-yl)-pyrimidin-2-ylamino]-benzenesulfonamide (**2**). By condensation of 3-dimethylamino-1-(2-ethylamino-4-methyl-thiazol-5-yl)-propenone and nitrate of 3-guanidino-benzenesulfonamide. Yellow solid; mp: 148-150 °C; anal. RP-HPLC (0-60% MeCN): t_R = 13.1 min; ^{1}H-NMR (500 MHz, DMSO-d_6): δ 1.18 (t, J = 7.5 Hz, 3H), 2.48 (s, 3H), 3.27 (m, 2H), 6.94 (d, J = 6.0 Hz, 1H), 7.39 (m, 1H), 7.45 (m, 1H), 7.94 (m, 1H), 8.10 (m, 2H), 8.32 (s, 1H), 8.35 (d, J = 5.5 Hz, 1H), 9.74 (s, 1H); ^{13}C-NMR (125 MHz, DMSO-d_6): δ 14.98, 19.39, 108.13, 116.27, 117.98, 118.89, 122.22, 129.64, 141.78, 145.19, 153.46, 158.25, 159.48, 159.96, 169.45; HRMS (*m/z*): $[M+H]^+$ calcd for $C_{16}H_{19}N_6O_2S_2$, 391.1011; found, 391.1007.

3-[4-(4-Methyl-2-methylamino-thiazol-5-yl)-pyrimidin-2-ylamino]-benzenesulfonamide (**3**). By condensation of 3-dimethylamino-1-(4-methyl-2-methylamino-thiazol-5-yl)-propenone and nitrate of 3-guanidino-benzenesulfonamide. Yellow solid; mp: 276-278 °C; anal. RP-HPLC (0-60% MeCN): t_R = 11.8 min; ^{1}H-NMR (500 MHz, DMSO-d_6): δ 2.73 (s, 3H), 3.12 (d, , J = 5.0 Hz, 3H), 7.20 (d, J = 6.0 Hz, 1H), 7.52 (s, 2H), 7.65 (d, J = 8.0 Hz, 1H), 7.70 (t, J = 8.0 Hz, 1H), 8.18 (d, J = 8.0 Hz, 1H), 8.29 (m, 1H), 8.59 (br s, 1H), 8.61 (d, J = 6.0 Hz, 1H); ^{13}C-NMR (125 MHz, DMSO-d_6): δ 19.8, 31.9, 107.98, 112.50, 116.33, 118.32, 119.01, 122.22, 129.64, 141.77, 145.20, 153.52, 158.28, 159.45, 159.95; HRMS (*m/z*): $[M+H]^+$ calcd for $C_{15}H_{17}N_6O_2S_2$, 377.0854; found, 377.0857.

N-Methyl-3-[4-(4-methyl-2-methylamino-thiazol-5-yl)-pyrimidin-2-ylamino]-benzenesulfonamide (**4**). By condensation of 3-dimethylamino-1-(4-methyl-2-methylamino-thiazol-5-yl)-propenone and nitrate of 3-guanidino-*N*-methyl-benzenesulfonamide. Yellow solid; mp: 243-245 °C; anal. RP-HPLC (0-60% MeCN): t_R = 13.2 min; ^{1}H-NMR (500 MHz, DMSO-d_6): δ 2.53 (s, 3H), 2.57 (d, J = 5.0 Hz, 3H), 2.99 (s, 3H), 7.00 (d, J = 5.5 Hz, 1H), 7.44 (d, J = 8.0Hz, 1H), 7.48 (t, J = 8.0 Hz, 1H), 7.80 (d, J = 8.0 Hz, 1H), 8.33 (d, J = 5.5 Hz, 1H), 8.52 (s, 1H); ^{13}C-NMR (125 MHz, DMSO-d_6): δ 19.34, 29.46, 31.63, 108.08, 117.12, 118.29, 119.51, 122.66, 129.89, 140.35, 142.01, 153.54, 158.28,

159.40, 159.87, 170.47. HRMS (*m/z*): $[M+H]^+$ calcd for $C_{16}H_{19}N_6O_2S_2$, 391.1011; found, 391.1007.

3-[4-(2-Amino-4-methyl-thiazol-5-yl)-pyrimidin-2-ylamino]-N-methyl-benzenesulfonamide (**5**). By condensation of 1-(2-amino-4-methyl-thiazol-5-yl)-3-dimethylamino-propenone and nitrate of 3-guanidino-*N*-methyl-benzenesulfonamide. Yellow solid; mp: 206-208 °C; anal. RP-HPLC (0-60% MeCN: t_R = 15.9 min; ^{1}H-NMR (500 MHz, DMSO-d_6): δ 2.43 (s, 3H), 2.44 (s, 3H), 7.14 (d, J = 5.5 Hz, 1H), 7.35 (m, 1H), 7.52 (t, J = 8.0 Hz, 1H), 7.98 (d, J = 8.0 Hz, 1H), 8.30 (s, 1H), 8.58 (d, J = 5.5 Hz, 1H); ^{13}C-NMR (125 MHz, DMSO-d_6): δ 18.54, 19.65, 29.43, 109.85, 117.40, 119.91, 122.89, 130.02, 131.14, 140.40, 141.65, 152.98, 158.74, 160.07, 167.22; HRMS (*m/z*): $[M]^+$ calcd for $C_{15}H_{16}N_6O_2S_2$, 376.0776; found, 376.0774.

(3-Methanesulfonyl-phenyl)-[4-(4-methyl-2-methylamino-thiazol-5-yl)-pyrimidin-2-yl]-amine (**6**). By condensation of 3-dimethylamino-1-(4-methyl-2-methylamino-thiazol-5-yl)-propenone and *N*-(3-methanesulfonyl-phenyl)-guanidine nitrate. Light yellow solid; mp: 272-274 °C; anal. RP-HPLC (0-60% MeCN): t_R = 13.8 min; ^{1}H-NMR (500 MHz, DMSO-d_6): δ 2.86 (s, 3H), 2.87 (s, 3H), 3.20 (s, 3H), 6.98 (d, J = 5.5 Hz, 1H), 7.46 (d, J = 7.5 Hz, 1H), 7.54 (t, J = 7.5 Hz, 1H), 7.95 (m, 1H), 8.08 (m, 1H), 8.38 (d, J = 5.0 Hz, 1H), 8.54 (s, 1H), 9.87 (s, 1H); ^{13}C-NMR (125 MHz, DMSO-d_6): **δ** 19.33, 31.69, 44.47, 108.11, 116.72, 118.29, 119.77, 123.78, 130.15, 141.87, 142.24, 153.64, 158.37, 159.29, 159.78, 161.53; HRMS (*m/z*): $[M+H]^+$ calcd for $C_{16}H_{18}N_5O_2S_2$, 376.0902; found, 376.0902.

[4-(2-Ethylamino-4-methyl-thiazol-5-yl)-pyrimidin-2-yl]-(3-methanesulfonyl-phenyl)-amine (**7**). By condensation of 3-dimethylamino-1-(2-ethylamino-4-methyl-thiazol-5-yl)-propenone and *N*-(3-methanesulfonyl-phenyl)-guanidine nitrate. Light yellow solid; mp: 220-221 °C; anal. RP-HPLC (0-60% MeCN): t_R = 14.6 min; ^{1}H-NMR (500 MHz, DMSO-d_6): δ 1.19 (t, J = 7.0 Hz, 3H), 2.48 (s, 3H), 2.63-3.17 (m, 5H), 6.97 (d, J = 5.5 Hz, 1H), 7.47 (d, J = 7.5 Hz, 1H), 7.52 (t, J = 7.5 Hz, 1H), 7.94 (m, 1H), 8.16 (m, 1H), 8.38 (d, J = 5.0 Hz, 1H), 8.51 (s, 1H), 9.86 (s, 1H); ^{13}C-NMR (125 MHz, DMSO-d_6): δ 14.93, 19.36, 44.48, 46.00, 108.19, 116.74, 117.94, 119.78, 123.80, 130.17, 141.87, 142.27, 153.60, 158.34, 159.35, 159.80, 169.51; HRMS (*m/z*): $[M+H]^+$ calcd for $C_{17}H_{20}N_5O_2S_2$, 390.1058; found, 390.1060.

3-[4-(2-Amino-4-methyl-thiazol-5-yl)-pyrimidin-2-ylamino]-N-ethyl-benzenesulfonamide (**8**). By condensation of 1-(2-amino-4-methyl-thiazol-5-yl)-3-dimethylamino-propenone and nitrate of *N*-ethyl-3-guanidino-benzenesulfonamide. Yellow solid; mp: 176-177 °C; anal. RP-HPLC (0-60 % MeCN%): t_R = 13.5 min; ^{1}H-NMR (500 MHz, DMSO-d_6): δ 1.08 (t, J = 7.5 Hz, 3H), 2.51 (s, 3H), 2.95 (m, 2H), 6.98 (d, J = 5.5 Hz, 1H), 7.44-7.49 (m, 2H), 7.89 (d, J = 7.5 Hz, 1H), 8.34 (d, J = 5.5 Hz, 1H), 8.37 (br s, 1H); HRMS (*m/z*): $[M+H]^+$ calcd for $C_{16}H_{19}N_6O_2S_2$, 391.1011; found, 391.1007.

[4-(4-Methyl-2-methylamino-thiazol-5-yl)-pyrimidin-2-yl]-[4-methyl-3-(morpholine-4-sulfonyl)-phenyl]-amine (**9**). By condensation of 3-dimethylamino-1-(4-methyl-2-methylamino-thiazol-5-yl)-propenone and *N*-[4-methyl-3-(morpholine-4-sulfonyl)-phenyl]-guanidine nitrate. Light yellow solid; mp: 237-238 °C; anal. RP-HPLC (0-60% MeCN): t_R = 15.8 min; ^{1}H-NMR (500 MHz, DMSO-d_6): δ 2.53 (s, 3H), 2.59 (s, 3H), 2.99 (s, 3H), 3.16 (m, 4H), 3.70 (m, 4H), 6.97 (d, J = 5.5 Hz, 1H), 7.34 (d, J = 8.0 Hz, 1H), 7.80 (d, J = 8.0 Hz, 1H), 8.31 (d, J = 5.0 Hz, 1H), 8.41 (s, 1H); ^{13}C-NMR (125 MHz, DMSO-d_6): δ 19.38, 20.38, 31.61, 46.03, 66.30, 108.02, 118.29, 119.89, 123.51, 129.75, 133.71, 135.34, 139.74, 153.47, 158.27, 159.50, 159.94, 170.38. HRMS (*m/z*): $[M+H]^+$ calcd for $C_{20}H_{25}N_6O_3S_2$, 461.1430; found, 461.1433.

[4-(2-Amino-4-methyl-thiazol-5-yl)-pyrimidin-2-yl]-[4-methyl-3-(morpholine-4-sulfonyl)-phenyl]-amine (**10**). By condensation of 1-(2-amino-4-methyl-thiazol-5-yl)-3-dimethylamino-propenone and *N*-[4-methyl-3-(morpholine-4-sulfonyl)-phenyl]-guanidine nitrate. Light yellow solid; mp: 183-184 °C; anal. RP-HPLC (0-60% MeCN): t_R = 15.5 min. ^{1}H-NMR (500 MHz, DMSO-d_6): δ 2.76 (s, 3H), 2.82 (s, 3H), 3.38 (m, 4H), 3.95 (m, 4H), 7.23 (d, J = 5.5 Hz, 1H), 7.66 (d, J = 9.0 Hz, 1H), 7.83 (s, 2H), 8.41 (m, 1H), 8.66

(d, *J* = 5.0 Hz, 1H); ^{13}C-NMR (125 MHz, DMSO-d_6): *δ* 19.16, 20.33, 46.03, 66.32, 108.31, 118.33, 120.11, 123.47, 129.70, 133.66, 135.41, 139.72, 153.12, 158.24, 159.63, 159.95, 169.62. HRMS (*m/z*): $[M+H]^+$ calcd for $C_{19}H_{23}N_6O_3S_2$, 447.1273; found 447.1271.

4-[4-(3,4-Dimethyl-2-oxo-2,3-dihydro-thiazol-5-yl)-pyrimidin-2-ylamino]-N-(2-methoxy-ethyl)-benzenesulfonamide (**11**). By condensation of 5-(3-dimethylamino-acryloyl)-3,4-dimethyl-3*H*-thiazol-2-one and nitrate of 4-guanidino-*N*-(2-methoxy-ethyl)-benzenesulfonamide; Yellow solid; mp: 238-239 °C; anal. RP-HPLC (0-60% MeCN): t_R = 16.3 min; ^{1}H-NMR (500 MHz, DMSO-d_6): *δ* 2.52 (s, 3H), 2.82 (q, *J* = 6.0, 12.0 Hz, 2H), 3.10 (s, 3H), 3.23 (m, 2H), 3.25 (s, CH_3), 7.00 (d, *J* = 5.5 Hz, 1H), 7.43 (t, *J* = 6.0 Hz, 1H), 7.64 (d, *J* = 9.0 Hz, 2H), 7.87 (d, *J* = 9.0 Hz, 2H), 8.44 (d, *J* = 5.5 Hz, 1H); ^{13}C-NMR (125 MHz, DMSO-d_6): *δ* 15.02, 30.35, 42.83, 58.56, 71.25, 110.08, 110.24, 118.85, 128.12, 133.08, 139.03, 144.63, 158.61, 159.30, 159.77, 170.37; HRMS (*m/z*): $[M+H]^+$ calcd for $C_{18}H_{22}N_5O_4S_2$, 436.1113; found 436.1111.

3-[4-(3,4-Dimethyl-2-oxo-2,3-dihydro-thiazol-5-yl)-pyrimidin-2-ylamino]-benzonitrile (**12**). By treatment of 5-(3-dimethylamino-acryloyl)-3,4-dimethyl-3*H*-thiazol-2-one and *N*-(3-cyano-phenyl)-guanidine nitrate; anal. RP-HPLC (10-70% MeCN): t_R = 15.5 min; ^{1}H-NMR (500 MHz, DMSO-d_6): *δ* 2.52 (s, 3H), 3.29 (s, 3H), 7.06 (d, *J* = 5.5 Hz, 1H), 7.40 (m, 1H), 7.51 (t, *J* = 8.0 Hz, 1H), 7.93 (m, 1H), 8.33 (s, 1H), 8.50 (d, *J* = 5.5 Hz, 1H), 10.00 (s, 1H); ^{13}C-NMR (125 MHz, DMSO-d_6): *δ* 14.97, 30.32, 109.94, 109.95, 112.05, 119.76, 121.89, 124.04, 125.43, 130.61, 139.02, 141.91, 158.55, 159.34, 159.78, 170.36; HRMS (*m/z*): $[M+H]^+$ calcd for $C_{16}H_{14}N_5OS$, 324.0919; found 324.0927.

3,4-Dimethyl-5-[2-(4-methyl-3-nitro-phenylamino)-pyrimidin-4-yl]-3H-thiazol-2-one (**13**). By condensation of 5-(3-dimethylamino-acryloyl)-3,4-dimethyl-3*H*-thiazol-2-one and *N*-(3-cyano-4-methyl-phenyl)-guanidine nitrate; anal. RP-HPLC (10-70% MeCN): t_R = 17.6 min; ^{1}H-NMR (500 MHz, DMSO-d_6): *δ* 2.44 (s, 3H), 2.55 (s, 3H), 3.28 (s, 3H), 7.03 (d, *J* = 5.5 Hz, 1H), 7.40 (d, *J* = 9.0 Hz, 1H), 7.84 (d, *J* = 9.0 Hz, 1H), 8.48 (d, *J* = 5.5 Hz, 1H,), 8.59 (s, 1H), 9.99 (s, 1H); ^{13}C-NMR (125 MHz, DMSO-d_6): *δ* 14.96, 19.70, 30.32, 109.79, 114.22, 124.13, 125.63, 133.42, 138.94, 140.07, 149.44, 158.54, 159.33, 159.80, 170.41; HRMS (*m/z*): $[M+H]^+$ calcd for $C_{16}H_{16}N_5O_3S$, 358.0974; found, 358.0976.

3,4-Dimethyl-5-[2-(4-piperazin-1-yl-phenylamino)-pyrimidin-4-yl]-3H-thiazol-2-one (**14**). A solution of potassium thiocyanate (5.67 g, 58 mmol) in Me_2CO (45 mL) was cooled on ice and 3-chloro-pentane-2,4-dione (6.95 mL, 58 mmol) was added dropwise. The mixture was warmed to room temperature and stirred for 6 h. After evaporation to dryness, the residue was dissolved in EtOH (30 mL) and conc. aq HCl (15 mL) was added. This mixture was heated to reflux for 14 h. After cooling, it was concentrated and the resulting precipitates were filtered and washed successively with cold MeOH and Et_2O to afford 5-acetyl-4-methyl-3*H*-thiazol-2-one (9.1 g, 100%). mp 208-211 °C; anal. RP-HPLC (10-70% MeCN): t_R = 6.5 min; ^{1}H-NMR (500 MHz, $CDCl_3$): *δ* 2.33 (s, 3H), 2.38 (s, 3H), 11.9 (s, 1H); ^{13}C-NMR (125 MHz, DMSO-d_6): *δ* 15.06, 29.94, 115.53, 142.99, 170.92, 189.91; FTIR: 3094, 2850, 1669, 1622, 1579 cm^{-1}; MS (*m/z*): $[M+H]^+$ calcd for $C_6H_8NO_2S$, 158.19; found 157.77.

5-Acetyl-4-methyl-3*H*-thiazol-2-one (4.64 g, 27.1 mmol) and *N*,*N*-dimethylformamide dimethylacetal (8.4 mL, 59.6 mmol) were mixed in a dry, Ar-flushed flask, and the mixture was heated at 100 °C for 3 h. After cooling, an equal volume of Et_2O was added. The resulting orange solid was filtered and washed with Et_2O to afford 2.73 g of 5-(3-dimethylamino-acryloyl)-3,4-dimethyl-3*H*-thiazol-2-one as an orange solid. ^{1}H-NMR (500 MHz, DMSO-d_6): *δ* 2.52 (s, 3H), 2.82 (br s, 3H), 3.11 (br s, 3H), 3.22 (s, 3H), 5.10 (d, *J* = 12.2Hz, 1H,), 7.61 (d, *J* = 11.7 Hz, 1H).

N-[4-(4-Acetyl-piperazin-1-yl)-phenyl]-guanidine nitrate was prepared following the procedures described previously (Wang et al., 2004a). The reaction mixture was filtered through Celite and concentrated under reduced pressure. Recrystallisation from EtOH

gave the pure product as a pale pink solid (91%). ^{1}H-NMR (500 MHz, DMSO-d_6): δ 2.06 (s, 3H), 3.15 (m, 4H), 3.58 (m, 4H), 7.04-7.19 (m, 8H), 9.32 (s, 1H).

A solution of 5-(3-dimethylamino-acryloyl)-3,4-dimethyl-3*H*-thiazol-2-one (0.20 g, 0.88 mmol), *N*-[4-(4-acetyl-piperazin-1-yl)-phenyl]-guanidine nitrate (0.38 g, 1.15 mmol) and NaOH (0.09 g, 2.3 mmol) in 2-methoxylethanol (15 mL) was heated at 120 °C for 20 h. The reaction mixture was evaporated to dryness and the residue was purified by silica gel chromatography, eluting with CH_2Cl_2, then 2% MeOH/CH_2Cl_2 to afford 5-[2-[4-(4-acetyl-piperazin-1-yl)-phenylamino]-pyrimidin-4-yl]-3,4-dimethyl-3*H*-thiazol-2-one as a yellow solid (0.22 g, 60 %). Mp. 231-234 °C; anal. RP-HPLC (10-70% MeCN): t_R = 9.5 min; ^{1}H-NMR (500 MHz, DMSO-d_6): δ 2.03 (s, 3H), 2.55 (s, 3H), 3.01 (m, 2H), 3.08 (m, 2H), 3.29 (s, 3H), 3.57 (m, 4H), 6.87 (d, J = 5.5 Hz, 1H), 6.93 (d, J = 9.0 Hz, 2H), 7.58 (d, J = 9.0 Hz, 2H), 8.37 (d, J = 5.5 Hz, 1H), 9.37 (s, 1H); Analysis (calcd, found for $C_{21}H_{24}N_6O_2S$): C (58.41, 58.49), H (5.70, 5.77), N (19.80, 19.33).

This material, in 2 M HCl in EtOH, was heated under reflux for 2.5 h. After cooling, the mixture was evaporated, the residue was basified by addition of 2 M aq NaOH and extracted (2 × 50 mL CH_2Cl_2). The combined extracts were washed with brine, dried on $MgSO_4$, and filtered. The solvent was evaporated and the residue was crystallised from MeOH to afford 3,4-dimethyl-5-[2-(4-piperazin-1-yl-phenylamino)-pyrimidin-4-yl]-3*H*-thiazol-2-one (**14**) as a yellow solid (90%). mp. 224-226 °C; anal. RP-HPLC (0-60% MeCN): t_R = 10.9 min; ^{1}H-NMR (500 MHz, DMSO-d_6): δ 2.57 (s, 3H), 3.10 (m, 4H), 3.16 (m, 4H), 3.36 (s, 3H), 6.65 (d, J = 5.5 Hz, 1H), 6.94 (d, J = 10.5 Hz, 2H), 7.47 (d, J = 9.0 Hz, 2H), 8.31 (d, J = 5.5 Hz, 1H); ^{13}C-NMR (125 MHz, DMSO-d_6): δ 14.85, 30.20, 46.35, 50.84, 108.18, 110.62, 116.36, 121.11, 132.83, 138.18, 147.69, 158.38, 159.13, 160.33, 170.42. Analysis (calcd, found for $C_{19}H_{22}N_6OS \cdot 0.45\ H_2O$): C (59.55, 59.32), H (6.10, 6.14), N (25.59, 24.97).

Cloning, expression, and purification of His-tagged CDK9/Cyclin T1

Cloning and expression of His-tagged CDK9/cyclin T1. Baculoviral transfer vector pFastBac HTa (Invitrogen, Carlsbad, USA) was modified to produce pSSP1, by replacing the region between the *Rsr* II and *Eco* RI restriction endonuclease sites of pFastBac HTa with a double stranded linker corresponding to sense strand 5'-GTCCGTCCGAAACCAT GTCGTACTACCATCACCATCACCATCACGGTATGGCTAGCGACGATGACGATAAGGGATCCGTGC GGCCGCG-3'. This modification was introduced to allow expression of fusion proteins where the N-terminal polyhistidine tag (His-tag) could be removed by cleavage at an entertokinase cleavage site introduced immediately adjacent to the polypeptide encoded by the inserted gene of interest.

The CDK9 open reading frame was amplified from a human foetal lung 5'-Stretch Plus cDNA library (Clontech, Palo Alto, USA) using PCR primer 1 (5'-GCGTTGGAGGCGGCCATG GCAAAGCAGTACG-3') and 2 (5'-CTAGTGGCAAGCGCCGGCCCTCAGAAG-3'). The amplified DNA fragment was cloned into pCR4-Topo (Invitrogen, Carlsbad, USA), to give pCR4-CDK9. PCR primer 3 (5'-GGCGCTAGCGACGATGACGATAAGATGGCAAAGCAGTACGACTCG-3') and 4 (5'-CAGGAAACAGCTATGAC-3') were used to amplify the CDK9 open reading frame from pCR4-CDK9. The PCR product generated was digested with *Nhe* I and *Eco* RI and ligated into pSSP1, also digested with *Nhe* I and *Eco* RI. Insert DNA from several clones was sequenced, and fragment exchange was used to generate a single clone, pSSP1-Cdk9 with the correct CDK9 coding sequence.

The cyclin T1 open reading frame was amplified as two fragments from a human foetal lung 5'-Stretch Plus cDNA library (Clontech, Palo Alto, USA), using PCR primer 5 (5'-ATGGAGGGAGAGAGGAAGAACAACAACAAACGGTGGTAT-3') and 6 (5'-GTAAGTGCTAAATTC TCACTAGTCCG-3'), or PCR primer 7 (5'-CTACTCAGGG TCATCGGACT AGTGAG-3') and 8 (5'-TTACTTAGGAAGGGGTGGAAGTGGTGGAGGAGGTTCTGA-3'). Each of the PCR products generated were cloned into pCR4-Topo, giving pCR4-5'Cyclin T1 and pCR4-3'cyclin T1, respectively. The sequence of these PCR fragments was confirmed. The cyclin T1 fragment of pCR4-5'cyclin T1 was then amplified using PCR primer 9 (5'-

GGCGCTAGCGACGATGACGATAAGATGGAGGGAGAGAGGAAGAACAAC-3') and 4 (5-CAGGA AACAGCTATGAC-3'), to introduce an *Nhe* I restriction endonuclease site upstream of the Cyclin T1 coding sequence. The resulting PCR product was digested with *Nhe* I and *Eco* RI and then ligated into pSSP1, also digested with *Nhe* I and *Eco* RI, to give pSSP-5'cyclin T1. The complete cyclin T1 open reading frame was subsequently generated by digesting pCR4-3'cyclin T1 with *Not* I and *Spe* I, and ligating the required fragment into pSSP-5'cyclin T1, also digested with *Not* I and *Spe* I, to create pSSP1-cyclin T1.

Bacmid DNA and baculoviral stocks were generated from pSSP1-CDK9 and pSSP1-cyclin T1 according to the manufacturer's instructions for pFastBac HTa. High-titre baculoviral stocks were generated by amplification in Sf9 cells grown in suspension culture. Viral titres were determined by standard plaque assay protocols, as per the manufacturer's instructions.

His-tagged CDK9 and cyclin T1 were co-expressed following co-infection of Sf9 cells by SSP1-CDK9 and SSP1-cyclin T1 baculoviruses. 72 h post-infection, cells were harvested by centrifugation, and snap frozen. Recombinant protein expression levels were confirmed by western blotting, using CDK9 sc-8338 and cyclinT1 sc-10750 antibodies (Santa Cruz Biotechnology, Inc., Santa Cruz, USA).

Protein Purification. The Sf9 cell pellet from 300 mL cell culture was lysed in 30 mL of 25 mM HEPES pH 7.5, 0.02 mM EGTA, 0.02 mM EDTA, 270 mM sucrose, 1% Triton X-100, 0.07% β-mercaptoethanol, 1 mM Na_3VO_4, 5 mM NaF, 0.2 mM PMSF, 1 mM benzamidine, protease inhibitor cocktail (Sigma, St. Louis, USA). After incubating on ice for 20 min, the samples were cleared by centrifuging for 20 min at 15,000 rpm. The resulting supernatant was supplemented with NaCl to 0.3 M, and then 1.2 mL (pre-equilibrated) Ni-NTA beads were added. After 1.5 h constant rotation at 4 ^{o}C, samples were centrifuged for 2 min at 2,000 rpm and supernatant was removed. Beads were re-suspended in 10 mL of 25 mM HEPES pH 7.5, 0.02 mM EGTA, 0.02 mM EDTA, 0.5 M NaCl, 20 mM imidazole, 0.03% Brij-35, 0.07% β-mercaptoethanol, 0.2 mM PMSF, 1 mM benzamidine then and transferred to a 12 mL column. Washing was performed twice with 10 mL of 25 mM HEPES pH 7.5, 0.02 mM EGTA, 0.02 mM EDTA, 0.5 M NaCl, 20 mM imidazole, 0.03% Brij-35, 0.07% β-mercaptoethanol, 0.2 mM PMSF, 1 mM benzamidine, and then twice with 10 mL of 25 mM HEPES pH 7.5, 0.02 mM EGTA, 0.02 mM EDTA, 0.3 M NaCl, 0.03% Brij-35, 0.07% β-mercaptoethanol, 0.2 mM PMSF, 1 mM benzamidine. CDK9/cyclin T1 was eluted with three washes of 2 mL of 25 mM HEPES pH 7.5, 0.02 mM EGTA, 0.02 mM EDTA, 0.3 M NaCl, 0.03% Brij-35, 0.07% β-mercaptoethanol, 0.2 mM PMSF, 1 mM benzamidine, 200 mM imidazole. CDK9/cyclin T1-containing fractions were identified by Western blotting. These fractions were combined and then dialysed overnight against 100 volumes of 50 mM Tris/HCl pH7.5, 0.1 mM EGTA, 150 mM NaCl, 270 mM sucrose, 0.03% Brij-35, 0.07% β-mercaptoethanol, 1 mM benzamidine, 0.1 mM PMSF. Protein concentration was determined by BCA assay. Samples were snap frozen in 100 µL aliquots, and stored at -70 °C. Specific activity was determined prior to use in screening assays.

Biopharmaceutical profiling and PK determinations

Test compound partitioning between octanol and aqueous buffer was carried out using the shake-flask method (Dearden, 1985). Compound pK_a values were determined using a pH-metric titration method (GlpKa; Sirius) (Comer, 2003). Aqueous solubility was assessed by turbidimetric measurements (Brooker et al., 1974). Apparent permeability coefficients were measured using a Caco-2 cell layer assay (Gan et al., 1997). *In vitro* phase-I liver metabolism was assessed by disappearance of parent compound (LC-MS quantitation) from a preparation of rat liver microsomes (Houston et al., 1997). Rat plasma protein binding was determined in an equilibrium dialysis assay (Kariv et al., 2001).

For PK measurements 3 male Wistar rats per sample and dose were treated by *iv* bolus injection or by *po* gavage of test compound solutions. Blood samples were collected

from each rat from the cannulated jugular vein at time zero and at intervals up to 24 h. Samples were centrifuged immediately and plasma was harvested and frozen at –20 °C until analysis. Quantitative compound level analysis was carried out using LC-MS/MS methods. PK parameters were derived by the noncompartmental methods using the WinNonlin 3.2 software programme (Pharsight). Oral bioavailability (%F) was calculated by taking the ratio of dose-normalised AUC values from oral *versus* parenteral dosing.

Evaluation of anti-tumour efficacy

Murine P388/0 leukaemia model. Six-week-old male CD2F1 mice were implanted intraperitoneally with P388/0 leukaemia cells (10^5) on day 0. On day 1 post-inoculation mice were given by *ip* administration either vehicle or test compound (0.1 mL / 10 g body weight) at the dose shown, on a treatment schedule of twice a day for 10 days. The effectiveness of treatment was assessed by comparison of the median post-inoculation lifespan (ILS) of each group of treated mice with that of the vehicle control group. The ILS ratio of the treated and control groups was used as an indicator of efficacy.

Colo-205 xenograft model. Female athymic ICR SCID mice, 5-6 weeks old on day 1 of the treatment, were used for this study. Test animal were implanted subcutaneously on day 0 with 30-60 mg tumour fragments using a 12-gauge trocar needle. Treatment began on day 18 when the mean estimated tumour mass for all groups in the study was 107 mg (range 97-115 mg). The animals were assigned into the treatment and the control groups with 10 mice per group. All animals were observed for clinical signs at least once daily. Tumour size was measured at least twice weekly. Animals were terminated at any time during the study if the tumour size became excessive or any adverse effects were noted. The treatments were administered by *ip* injection or *po* gavage daily, staring on day 18, and continuing for 8 days. The tumour burden (mg) was estimated from calliper measurements using the formula for the volume of a prolate ellipsoid assuming unit density. The mean tumour mass on the day of randomisation was reported for each group. Calculations of relative tumour mass and plot of mean tumour growth curves were performed. The relative tumour mass data from each group were compared using a one-way analysis of variance (ANOVA) and statistical significance was determined using the built-in data analysis tools in Microsoft Excel and R (The R Project for Statistical Computing).

Crystallography

Human recombinant CDK2 was expressed, purified, and crystallised as previously described (Wu et al., 2003). Data were collected at the Cyclacel home source with a FR-D X-ray generator using a Raxis IV++ image plate (Rigaku). Data processing was carried out using the d*TREK software suite (Pflugrath, 1999). The structures were solved by molecular replacement using MOLREP (Vagin et al., 1997) and PDB entry 1PW2. ARP/wARP (Lamzin et al., 1997) was used for initial density interpretation and the addition of water molecules. REFMAC (Murshudov et al., 1997) was used for structural refinement. A number of rounds of refinement and model building with the programme COOT (Emsley et al., 2010) were carried out. All the crystallographic programmes used were part of the *CCP4* programme suite (Potterton et al., 2004). The coordinates of the X-ray crystal structures of compounds **11** and **14** in complex with CDK2 have been deposited with the PDB (www.rcsb.org) under accession codes 2XMY and 2XNB.

Supplemental References

Brooker, P.J., and Ellison, M. (1974). Determination of the water solubility of organic compounds by a rapid turbidimetric method. Chem. Ind., 285-287.

Comer, J.E.A. (2003). High-throughput measurement of log D and pKa. Methods Principles Med. Chem. *18*, 21-45.

Dearden, J.C. (1985). Partitioning and lipophilicity in quantitative structure-activity relationships. Environ. Health Persp. *61*, 203-228.

Gan, L.-S.L., and Thakker, D.R. (1997). Applications of the Caco-2 model in the design and development of orally active drugs: elucidation of biochemical and physical barriers posed by the intestinal epithelium. Adv. Drug Delivery Rev. *23*, 77-98.

Houston, J.B., and Carlile, D.J. (1997). Prediction of hepatic clearance from microsomes, hepatocytes, and liver slices. Drug Metabol. Rev. *29*, 891-922.

Kariv, I., Cao, H., and Oldenburg, K.R. (2001). Development of a high throughput equilibrium dialysis method. J. Pharm. Sci. *90*, 580-587.

Lamzin, V.S., and Wilson, K.S. (1997). Automated refinement for protein crystallography. Methods Enzymol. *277*, 269-305.

Murshudov, G.N., Vagin, A.A., and Dodson, E.J. (1997). Refinement of macromolecular structures by the maximum-likelihood method. Acta Crystallogr. *D53*, 240-255.

Pflugrath, J.W. (1999). The finer things in X-ray diffraction data collection. Acta Crystallogr. *D55* 1718-1725.

Potterton, L., McNicholas, S., Krissinel, E., Gruber, J., Cowtan, K., Emsley, P., Murshudov, G.N., Cohen, S., Perrakis, A., and Noble, M. (2004). Developments in the CCP4 molecular-graphics project. Acta Crystallogr. *D60*, 2288-2294.

Vagin, A., and Teplyakov, A. (1997). MOLREP: an automated program for molecular replacement. J. Appl. Crystallogr. *30*, 1022 -1025.

Wang, S., Meades, C., Wood, G., Osnowski, A., Anderson, S., Yuill, R., Thomas, M., Mezna, M., Jackson, W., Midgley, C., Griffiths, G., Fleming, I., Green, S., McNae, I., Wu, S.-Y., McInnes, C., Zheleva, D., Walkinshaw, M.D., and Fischer, P.M. (2004a). 2-Anilino-4-(thiazol-5-yl)pyrimidine CDK Inhibitors: Synthesis, SAR analysis, X-Ray Crystallography, and Biological Activity. J. Med. Chem. *47*, 1662-1675.

Wang, S., Wood, G., Meades, C., Griffiths, G., Midgley, C., McNae, I., McInnes, C., Anderson, S., Jackson, W., Mezna, M., Yuill, R., Walkinshaw, M., and Fischer, P.M. (2004b). Synthesis and Biological Activity of 2-Anilino-4-(1H-pyrrol-3-yl)pyrimidine CDK Inhibitors. Bioorg. Med. Chem. Lett. *14*, 4237-4240.

Wu, S.Y., McNae, I., Kontopidis, G., McClue, S.J., McInnes, C., Stewart, K.J., Wang, S., Zheleva, D.I., Marriage, H., Lane, D.P., Taylor, P., Fischer, P.M., and Walkinshaw, M.D. (2003). Discovery of a Novel Family of CDK Inhibitors with the Program LIDAEUS: Structural Basis for Ligand-Induced Disordering of the Activation Loop. Structure *11*, 399-410.